Article

Structural Characterization and Biological Evaluation of Small Interfering RNAs Containing Cyclohexenyl Nucleosides

Koen Nauwelaerts, Michael Fisher, Matheus Froeyen, Eveline Lescrinier, Arthur Van Aerschot, Dong Xu, Robert DeLong, Hyumin Kang, Rudolph L. Juliano, and Piet Herdewijn

J. Am. Chem. Soc., **2007**, 129 (30), 9340-9348• DOI: 10.1021/ja067047q • Publication Date (Web): 06 July 2007

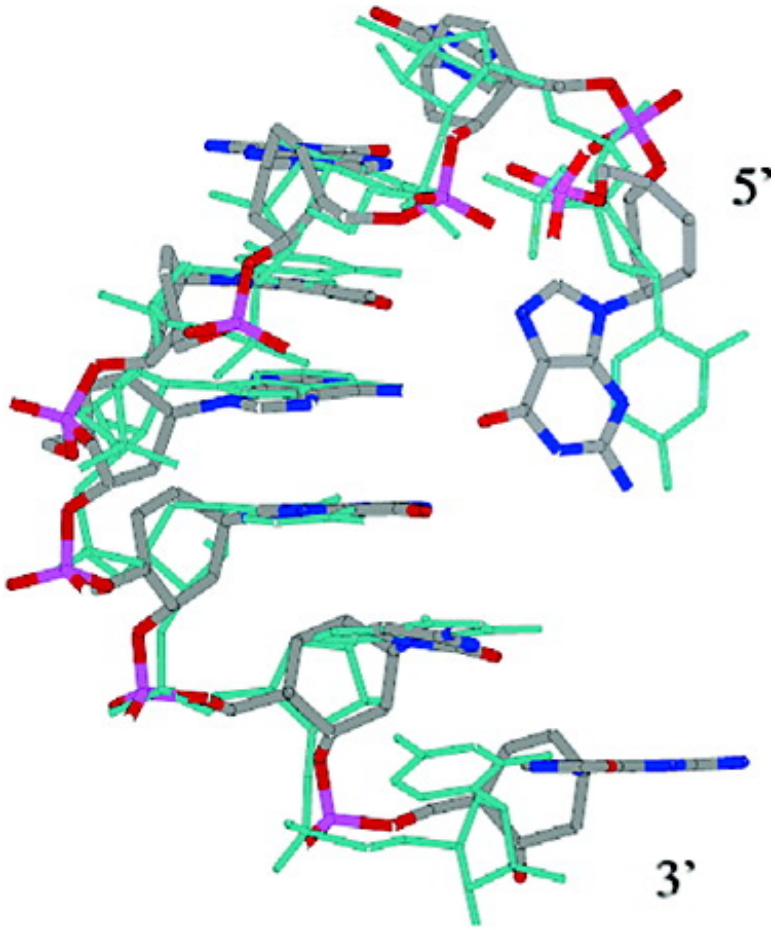

J|A|C|S
ARTICLES
Published on Web 07/06/2007

Structural Characterization and Biological Evaluation of Small Interfering RNAs Containing Cyclohexenyl Nucleosides

Koen Nauwelaerts,* Michael Fisher,† Matheus Froeyen,† Eveline Lescrinier,† Arthur Van Aerschot,† Dong Xu,‡ Robert DeLong,‡,§ Hyumin Kang,‡ Rudolph L. Juliano,‡ and Piet Herdewijn*,†

Contribution from the Laboratory of Medicinal Chemistry, Rega Institute for Medical Research, Minderbroedersstraat 10, B-3000 Leuven, Belgium, the Department of Pharmacology, School of Medicine, University of North Carolina, Chapel Hill, North Carolina 27599, and the Department of Chemistry and Physics, Virginia State University, Petersburg, Virginia 23806

Received October 2, 2006; E-mail: piet.herdewijn@rega.kuleuven.be

Abstract: CeNA is an oligonucleotide where the (deoxy)ribose sugars have been replaced by cyclohexenyl moieties. We have determined the NMR structure of a CeNA:RNA duplex and have modeled this duplex in the crystal structure of a PIWI protein. An N puckering of the ribose nucleosides, a $_2H^3$ conformation of the cyclohexenyl nucleosides, and an A-like helix conformation of the backbone, which deviates from the standard A-type helix by a larger twist and a smaller slide, are observed. The model of the CeNA:RNA duplex bound to the PIWI protein does not show major differences in the interaction of the guide CeNA with the protein when compared with dsRNA, suggesting that CeNA modified oligonucleotides might be useful as siRNAs. Incorporation of one or two CeNA units in the sense or antisense strands of dsRNA led to similar or enhanced activity compared to unmodified siRNAs. This was tested by targeting inhibition of expression of the MDR1 gene with accompanying changes in P-glycoprotein expression, drug transport, and drug resistance.

1. Introduction

In searching for oligonucleotides that can mimic the function of RNA but with increased enzymatic and chemical stability, we have developed cyclohexenyl nucleic acids (CeNA).[1−8] Although CeNA (Figure 1) is a deoxyoligonucleotide (it has no hydroxyl group in the position adjacent to the nucleobase), it resembles RNA in its conformational behavior. The monomers prefer to adopt a "Northern-type" conformation, and hybridization of CeNA is RNA selective (the stability of CeNA:RNA duplexes compared to CeNA:DNA duplexes is higher). Interesting properties of CeNA include its conformational flexibility, which means that a cyclohexenyl nucleoside can adapt its conformation to its chemical environment and its stability against enzymatic degradation. We have demonstrated that a cyclohexenyl nucleotide can adopt a "Southern-type" or a "Northern-type" conformation dependent on the number and the position of incorporated CeNA units in duplex oligonucleotide sequences. Therefore CeNA might be a good candidate to be tested as an RNA mimic in biological experiments. This may be of particular interest in the context of the regulation of gene expression by small interfering RNAs (siRNAs).

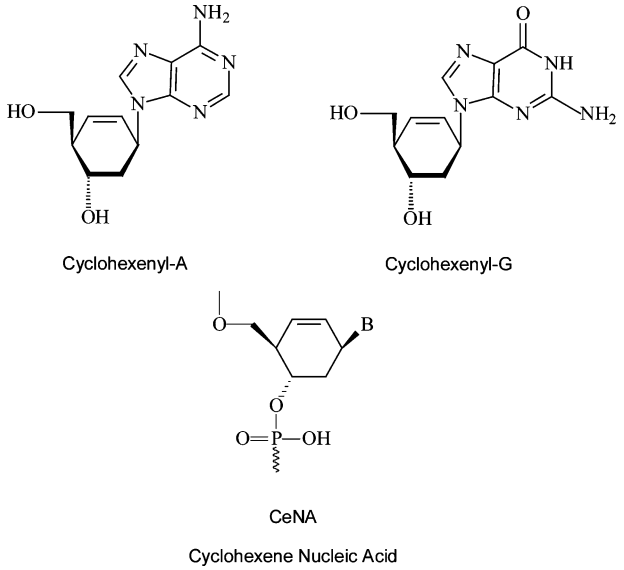

Figure 1. Structures of cyclohexenyl-A and cyclohexenyl-G which are used to synthesize cyclohexenyl nucleic acids (CeNA)−RNA hybrids.

† Rega Institute for Medical Research.
‡ University of North Carolina.
§ Virginia State University.

(1) Wang, J.; Herdewijn, P. *J. Org. Chem.* **1999**, *64*, 7820−7827.
(2) Wang, J.; Froeyen, M.; Hendrix, C.; Andrei, G.; Snoeck, R.; De Clercq, E.; Herdewijn, P. *J. Med. Chem.* **2000**, *43*, 736−745.
(3) Wang, J.; Verbeure, B.; Luyten, I.; Lescrinier, E.; Froeyen, M.; Hendrix, C.; Rosemeyer, H.; Seela, F.; Van Aerschot, A.; Herdewijn, P. *J. Am. Chem. Soc.* **2000**, *122*, 8595−8602.
(4) Wang, J.; Morral, J.; Hendrix, C.; Herdewijn, P. *J. Org. Chem.* **2001**, *66*, 8478−8482.
(5) Verbeure, B.; Lescrinier, E.; Wang, J.; Herdewijn, P. *Nucleic Acids Res.* **2001**, *29*, 4941−4947.
(6) Gu, P.; Schepers, G.; Rozenski, J.; Van Aerschot, A.; Herdewijn, P. *Oligonucleotides* **2003**, *13*, 479−489.
(7) Gu, P.; Griebel, C.; Van Aerschot, A.; Rozenski, J.; Busson, R.; Gais, H.-J.; Herdewijn, P. *Tetrahedron.* **2004**, *60*, 2121−2123.
(8) Nauwelaerts, K.; Lescrinier, E.; Sclep, G.; Herdewijn, P. *Nucleic Acids Res.* **2005**, *33*, 2452−2463.

10.1021/ja067047q CCC: $37.00

RNA interference (RNAi) is the process of posttranscriptional dsRNA-dependent gene silencing; it is a method of cellular defense and a regulatory mechanism for the expression of cellular genes.[9−11] Small interfering RNAs (siRNAs) are the mediators of targeted mRNA degradation,[12] and chemically synthesized siRNA duplexes are becoming a promising new tool in fundamental and clinical research.[13] The mechanism of gene silencing by dsRNA is highly complex and not fully understood.[14] It involves the formation of an RNA-induced silencing complex (RISC) that contains a member of the Argonaute protein family. In order to use siRNA therapeutically in mammalian organisms it will be important to increase the degree and persistence of gene silencing. A key aspect of this is that the extracellular and intracellular stability of the siRNA must be increased by chemical modifications.[15] For the chemically modified nucleotides that have been evaluated so far for siRNA applications, it is clear that the 2′-OH group of RNA is not absolutely necessary for RNAi activity.[16] However, the introduction of modifications such as 2′-O-methyl- or LNA (Locked Nucleic Acid) moieties must be restricted to certain regions of the siRNA sequence so as not to lose biological potency.[17−21] In introducing modifications, a balance needs to be found between increasing the stability to nuclease degradation while not losing biological activity. Thus far, 2′-deoxy-2′-fluoro nucleoside modifications seem to be the best choice as substitutes for ribonucleosides in siRNA.[16,10] The potency of siRNAs modified in the antisense strand ranks in the order 2′-F > 2′-OMe > 2′-OMOE [2′-O-(2-methoxyethyl)].[22] The sense strand is more tolerant to modification than the antisense strand. However, although a variety of modifications are tolerated, there is little evidence that even the best (2′-F) modified siRNAs are more potent *in vivo* than unmodified siRNA.[23]

When designing the modified RNA, some simple rules should be taken into consideration. More effective siRNA duplexes show reduced thermodynamic stability at the 5′-end of the antisense siRNA relative to the 3′-end within the duplex.[14] RISC cleaves the target mRNA in the middle of the complementary region, 10 nucleotides upstream of the nucleotide with the 5′-end of the guide siRNA,[24] yielding a 5′-phosphate and a 3′-hydroxyl termini.[25] Dicer cleaves long dsRNA into 21- to 28 nucleotide siRNA duplexes that contain 2 nucleotide 3′-overhangs with 5′-phosphate and 3′-hydroxyl termini.[14] Based on these observations, modifications at the 5′-end of the antisense siRNA that increase thermodynamic stability or impede 5′-O-phosphorylation,[26] and modifications in the middle of the duplex that will interfere with RNase cleavage, are more likely to reduce siRNA activity. It has been demonstrated that 2′-OMe and 2′-F modified nucleoside residues incorporated at the cleavage site do not interfere with nucleolytic activity.[22] For example, a recent publication describes the potent anti-HBV (Hepatitis B Virus) activity of fully modified siRNA (using 2′-OMe, 2′-F, and deoxynucleotides).[27]

ORF1

sense	5’-GUAUUGACAGCUAUUCGAAdTdT-3’
antisense	3’-dTdTCAUAACUGUCGAUAAGCUU-5’

ORF2

sense	5’-GAACUCUUAGCGUAUGCAAdTdT-3’
antisense	3’-dTdT CUUGAGAAUCGCAUACGUU

Figure 2. dsRNA sequences with two dT overhangs at the 3′-end, targeting the MDR1 gene (target regions designated ORF1 and ORF2).

In this paper we have investigated the physical and biological properties of RNA-like CeNA oligonucleotides. We have determined the solution structure of an RNA/CeNA duplex by NMR and have used computational approaches to evaluate the functional analogy between RNA and CeNA by analyzing the potential of CeNA to function as a substitute for RNA in siRNAs. We have also tested the effects of CeNA modifications on the potency of siRNAs using the human MDR1 gene as a target. The product of this gene is the P-glycoprotein, a transmembrane ATPase that confers resistance to a variety of antitumor drugs.[28] The anti-MDR1 siRNA sequences chosen are shown in Figure 2.

2. Materials and Methods

2.1. Oligonucleotides. The synthesis and characterization of all oligonucleotides that have been used in the experiments have been described previously.[3] All oligonucleotides were characterized using HPLC (Supporting Information), mass spectrometry (Table 3), and T_m measurements (Supporting Information).

2.2. NMR Sample Preparation. The duplex used for the NMR experiments [Ce(5′-GCGTAGCG-3′)/r(5′-CGCUACGC-3′)] was obtained by titrating an RNA solution r(5′-CGCUACGC-3′) with the complementary CeNA sequence Ce(5′-GCGTAGCG-3′). Structure and main torsion angles of the cyclohexenyl nucleosides are shown in Figure 3A and B. After titration, the pD of the sample was adjusted to 7.2. The sample was lyophilized and redissolved in 0.25 mL of D_2O, resulting in a concentration of 2.1 mM of the duplex. For spectra in H_2O, the sample was again lyophilized and dissolved in 0.25 mL of 90%H_2O/10%D_2O.

2.3. NMR Spectroscopy. Spectra were recorded on a Varian 500 Unity spectrometer (operating at 499.140 MHz). Unless stated otherwise, spectra were recorded at 15 °C. The solution structure of the duplex was determined using standard homonuclear and heteronuclear

(9) Fire, A.; Xu, S.; Montgomery, M. K.; Kostas, S. A.; Driver, S. E.; Mello, C. C. *Nature* **1998**, *391*, 806−811.
(10) Montgomery, M. K.; Fire, A. *Trends Genet.* **1998**, *14*, 255−258.
(11) Smardon, A.; Spoerke, J. M.; Stacey, S. C.; Klein, M. E.; Mackin, N.; Maine, E. M. *Curr. Biol.* **2004**, *10*, 169−178.
(12) Martinez, J.; Patkaniowska, A.; Urlaub, H.; Luhrmann, R.; Tuschl, T. *Cell* **2002**, *110*, 563−574.
(13) Tuschl, T. *Nat. Biotechnol.* **2002**, *20*, 446−448.
(14) Meister, G.; Tuschl, T. *Nature* **2004**, *431*, 343−349.
(15) Dorsett, Y.; Tuschl, T. *Nat. Rev. Drug Discov.* **2004**, *3*, 318−329.
(16) Chiu, Y. L.; Rana, T. M. *RNA* **2003**, *9*, 1034−1048.
(17) Amarzguioui, M.; Holen, T.; Babaie, E.; Prydz, H. *Nucleic Acids Res.* **2003**, *31*, 589−595.
(18) Holen, T.; Amarzguioui, M.; Babaie, E.; Prydz, H. *Nucleic Acids Res.* **2003**, *31*, 2401−2407.
(19) Braasch, D. A.; Jensen, S.; Liu, Y.; Kaur, K.; Arar, K.; White, M. A.; Corey, D. R. *Biochemistry* **2003**, *42*, 7967−7975.
(20) Elmén, J.; Thonberg, H.; Ljungberg, K.; Frieden, M.; Westergaard, M.; Xu, Y.; Wahren, B.; Liang, Z.; Orum, H.; Koch, T.; Wahlestedt, C. *Nucleic Acids Res.* **2005**, *33*, 439−447.
(21) Czauderna, F.; Fechtner, M.; Dames, S.; Aygun, H.; Klippel, A.; Pronk, G. J.; Giese, K.; Kaufmann, J. *Nucleic Acids Res.* **2003**, *31*, 2705−2716.
(22) Prakash, T. P.; Allerson, C. R.; Dande, P.; Vickers, T. A.; Sioufi, N.; Jarres, R.; Baker, B. F.; Swayze, E. E.; Griffey, R. H.; Bhat, B. *J. Med. Chem.* **2005**, *30*, 4247−4253.
(23) Manoharan, M. *Curr. Opin. Chem. Biol.* **2004**, *8*, 570−579.
(24) Elbashir, S. M.; Lendeckel, W.; Tuschl, T. *Genes Dev.* **2001**, *15*, 188−200.
(25) Martinez, J.; Tuschl, T. *Genes Dev.* **2004**, *18*, 975−980.
(26) Nykänen, A.; Haley, B.; Zamore, P. D. *Cell* **2001**, *107*, 309−321.
(27) Morrissey, D. V.; Lockridge, J. A.; Shaw, L.; Blanchard, K.; Jensen, K.; Breen, W.; Hartsough, K.; Machemer, L.; Radka, S.; Jadhav, V.; Vaish, N.; Zinnen, S.; Vargeese, C.; Bowman, K.; Shaffer, C. S.; Jeffs, L. B.; Judge, A.; MacLachlan, I.; Polisky, B. *Nat. Biotechnol.* **2005**, *23*, 1002−1007.
(28) Gottesman, M.; Fojo, T.; Bates, S. *Nat. Rev. Cancer* **2002**, *2*, 48−58.

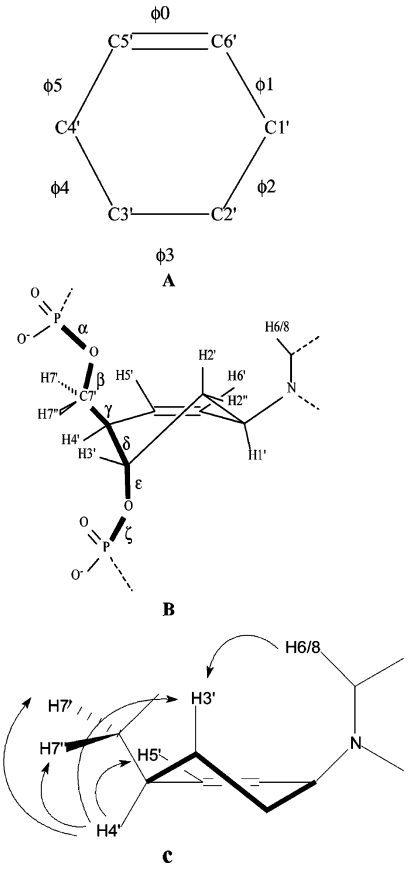

Figure 3. (A) Chemical structure and (B) main torsion angles of the cyclohexenyl nucleosides. (C) Important intraresidue NOE contacts in the cyclohexenyl nucleoside.

techniques.[29−38] Spectra were processed using the FELIX 97.00 software package (Biosym Technologies, San Diego, VA) running on a Silicon Graphics O2 R10000 workstation (IRIX version 6.3).

Nonexchangeable protons in the entire duplex could be assigned starting from a standard anomeric to aromatic proton walk. Sequential connectivities could be achieved in the RNA as well as in the CeNA strands of the duplex and provided assignments for H1′ H5, H6, and H8 protons. The other protons of the spin systems were assigned from TOCSY, DQF-COSY, and NOESY spectra.[39] The ^{31}P resonances were assigned from the 2D ^{1}H-detected [^{1}H,^{31}P] correlation spectrum. One-dimensional imino-proton spectra recorded at various temperatures in 90% H_2O/10% D_2O showed six sharp signals between 12.5 and 14 ppm. Due to fraying at the helix ends, imino signals of G1 and G8 could not be observed.

2.4. NMR Derived Restraints. 2.4.1. Distance Restraints. Distance restraints were derived from NOESY spectra recorded with 50, 100, and 150 ms mixing times. Based on the buildup curves, interproton distances were calculated. An experimental error (±20%) was used on the calculated interproton distances. The calibration of NOE cross-peak intensities was done against the H5−H6 cross-peaks as an internal standard. In the CeNA strand this resulted in 35 inter-residue and 120 intraresidue distance restraints, in the RNA strand 32 inter-residue and 56 intraresidue restraints could be obtained, and inter-strand NOE contacts with the H2 protons of both Adenine residues resulted in 6 interstrand restraints.

2.4.2. Puckering Restraints: Sugar puckers of the riboses in the RNA strand were inferred from the weak H1′ to H2′ (<2 Hz) scalar couplings and indicate N puckering of the sugar rings. In the CeNA strand, coupling constants in the cyclohexene rings were evaluated by fitting the H3′−H4′ and H4′−H5′ COSY cross-peaks with the ACME computer program.[40] An analysis of the obtained $J_{H2'-H3'}$ (3−4 Hz), $J_{H2''-H3'}$ (∼8−10 Hz), and $J_{H3'-H4'}$ (∼7−9 Hz) with the Hexrot computer program[8] shows the puckering of the cyclohexene rings to be $_2H^3$(N-Type) (72−93%). Very strong NOE contacts between H3′ and H6/H8 (2.01−2.77 Å) confirm these observations (Figure 3C). Dihedral restraints on O4′−C1′−C2′−C3′ (−25° ± 20°) and C1′−C2′−C3′−C4′ (37° ± 20°), to define the N-type ribose conformation, and on C1′−C2′−C3′−C4′ (59° ± 20°) and C2′−C3′−C4′−C5′ (−38° ± 20°), to define the $_2H^3$(N-Type) cyclohexene conformation, were used for the structure determination.

2.4.3. β Torsion Angle Restraints. The β torsion angles of the RNA and CeNA strands were restrained to the trans region (to 180° ± 30°) based on the observable four bond $J_{H4'-P(n)}$ couplings (∼4 Hz), indicating a W-shaped conformation of the atoms P−O5′−C5′−C4′. The small and almost equal coupling constants (∼3 Hz) which could be observed between P and H7′/H7″ in the CeNA strand and between P and H5′/H5″ in the RNA strand confirm these observations.

2.4.4. γ Torsion Angle Restraints. The small passive couplings observed in the H5′ to H5″ (RNA residues) cross-peaks in the DQF-COSY spectrum and the nicely resolved H4′-P(n) cross-peak in the 2D ^{1}H-detected [^{1}H,^{31}P] correlation spectrum allowed us to restrain the γ torsion angles in the RNA duplex to the $g+$ region (60° ± 35°). In the CeNA strand, close NOE contacts were observed between H7′ and H4′, H7″ and H4′, H7″ and H3′, and H7′ and H5′ (Figure 3C). Analysis of proton distances in the different possible conformations around the γ torsion angle shows that this pattern of NOE contacts corresponds to a $g+$ conformation, which was further supported by the nicely resolved H4′-P(n) cross-peak in the 2D ^{1}H-detected [^{1}H,^{31}P] correlation spectrum. The γ torsion angle of the CeNA residues was restrained to 60° ± 50°.

2.4.5. ϵ Torsion Angle Restraints. The ϵ torsion angles of the RNA residues were restrained (to 230° ± 70°) based on steric arguments. In the CeNA residues, no ϵ torsion angle constraints were applied. Other backbone angles were not restrained.

2.5. NMR Structure Calculation. All structure calculations of the Ce(5′-GCGTAGCG-3′)/r(5′-CGCUACGC-3′) duplex were performed with X-PLOR V3.851.[41] The topallhdg.dna and parallhdg.dna files were adapted to include the cyclohexenyl nucleotides (see Figure 4). In the topology file, 4 new CeNA residues were introduced (Ce−A, Ce−T, Ce−G, Ce−C). The modeled structure of a Ce−T monomer was used to derive energy constants. The torsion angle molecular dynamics protocol used was largely identical to that proposed for a DNA duplex.[42] A set of 100 structures was generated by torsion angle molecular dynamics, starting from two extended strands and using NMR derived restraints. After the torsion angle molecular dynamics round, the majority of the structures (65%) had converged to very similar structures with similar total energies (134−257 kcal mol^{-1}) and no violations of

(29) Wijmenga, S. S.; Mooren, M. M. W.; Hilbers, C. W. In *NMR of macromolecules: a practical approach*; Roberts, G. C. K., Ed.; Oxford University Press: Oxford, 1993.
(30) Wijmenga, S. S.; van Buuren, B. N. M. *Prog. Nucl. Magn. Reson. Spectrosc.* 1998, **32**, 287.
(31) States, D. J.; Haberkorn, R. A.; Ruben, D. J. *J. Magn. Reson.* **1982**, *48*, 286−292.
(32) Plateau, P.; Gueron, M. *J. Am. Chem. Soc.* **1982**, *104*, 7310−731.
(33) Piotto, M.; Saudek, V.; Sklenar, V. *J. Biomol. NMR* **1992**, *2*, 661−665.
(34) Rance, M.; Sorensen, O. W.; Bodenhausen, G.; Wagner, G.; Ernst, R. R.; Wuthrich, K. *Biochem. Biophys. Res. Commun.* **1983**, *117*, 479−485.
(35) Bax, A.; Davis, D. G. *J. Magn. Reson.* **1985**, *65*, 355−360.
(36) Jeener, J.; Meier, B. H.; Bachmann, P.; Ernst, R. R. *J. Chem. Phys.* **1979**, *71*, 4546−4553.
(37) Griesinger, C.; Otting, G.; Wuthrich, K.; Ernst, R. R. *J. Am. Chem. Soc.* **1988**, *110*, 7870−7872.
(38) Sklenar, V.; Miyashiro, H.; Zon, G.; Miles, H. T.; Bax, A. *FEBS Lett.* **1986**, *208*, 94−98.
(39) Lescrinier, E.; Esnouf, R.; Schraml, J.; Busson, R.; Heus, H.; Hilbers, C.; Herdewijn, P. *Chem. Biol.* **2000**, *7*, 719−731.
(40) Delaglio, F.; Wu, Z.; Bax, A. *J. Magn. Reson.* **2001**, *149*, 276−281.
(41) Schwieters, C. D.; Kuszewski, J. J.; Tjandra, N.; Clore, G. M. *J. Magn. Reson.* **2003**, *160*, 65−73.
(42) Stein, E. G.; Rice, L. M.; Brunger, A. T. *J. Magn. Reson.* **1997**, *124*, 154−164.

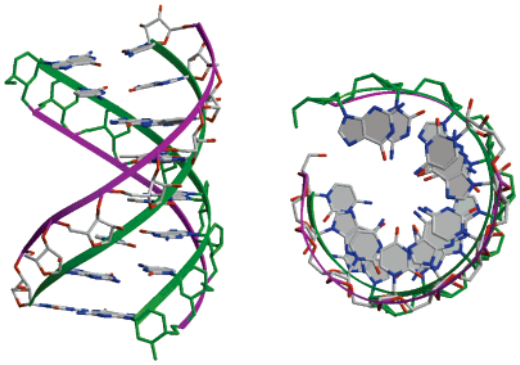

Figure 4. Visual representation of the structure closest to the average. The green strand is drawn through the C1′ carbons of all ribonucleosides and cyclohexenyl nucleosides. The purple strand interconnects the P atoms in both strands.

the NOE and dihedral restraints. The 25 lowest energy structures were used for further refinement during the "gentle molecular dynamics" round.

An analysis of the obtained 3D structure with the computer program X3DNA was used to measure torsion angles and helix parameters. Finally, some visual representations of the molecule were obtained with Molscript 1.4 and Bobscript 2.4.[43,44]

2.6. Molecular Modeling. Pictures are generated using Bobscript, Molscript, and Raster3d.[43−45]

2.6.1. Electrostatic Charges. Atomic electrostatic charges to be used in the amber software package were calculated from the electrostatic potential at the 6-31G* level using the package Gamess[46] and the two-stage RESP fitting procedure to account for the phosphate linkages.[47]

2.6.2. Amber Parameters. The force field parameters used in the amber simulations are those from the parm99 dataset.[48] Missing bond and angle parameters were taken from comparable bonds or angles from the AMBER force field. In particular, the parameters for the double bond in the sugar moiety were added. The Mn^{2+} metal parameters were also added.[49] This metal ion is contained in a highly conserved metal-binding site that anchors the 5′ nucleotide of the guide RNA.

2.6.3. Model Building. The modeling is based on the crystal structure of a PIWI protein in complex with a small siRNA:mRNA duplex (pdb structure file 2bgg)[50] and the NMR structure of an 8-mer duplex of CeNA:RNA (GCGTAGCG:CGCUACGC). This CeNA:RNA duplex is known to have an A-RNA-like conformation. The PIWI-bound siRNA:mRNA duplex was replaced by a CeNA:RNA duplex, by fitting the base atoms (N9 for purine, N1 for pyrimidine) by Quatfit (Quatfit program in CCL software archives). The CeNA strand was made to correspond to the siRNA strand. CeNA:RNA basepairs C2:G15 to G6:C11 have been fitted onto the central A-form helix part of the siRNA:mRNA duplex (base pairs U2:A13 to C6:G9). The unpaired 5′ U1 of mRNA was replaced by CeNA G1, and the unpaired end at the other side of siRNA G7C8 was replaced by CeNA residues C7G8 (see Supporting Information). The puckering of the 5′ CeNA nucleotide was set to a South conformation. The amber molecular mechanics energy of the system was minimized in the sander module of Amber 8.[51]

2.7. Cells. NIH 3T3 cells stably transfected with a plasmid containing the human *mdr1* gene were a gift from M. M. Gottesman. The NIH 3T3-MDR cells were grown in Dulbecco Modified Eagles Medium (DMEM-H) containing 10% Fetal Bovine Serum (FBS) and 60 ng/mL colchicine. The multidrug resistant cell line MES-Sa/DX-5 was obtained from the American Type Culture Collection; this uterine sarcoma fibroblast expresses high levels of MDR-1 mRNA and P-glycoprotein. The cells were grown in McCoy's medium containing 10% FBS and 60 ng/mL colchicine. Both cell lines were grown in a humidified atmosphere of 95% air and 5% CO_2 at 37 °C.

2.8. Treatment of Cells with siRNA Oligonucleotides. NIH 3T3-MDR cells were cultured in 185 mm flasks to 95% confluency and then seeded in 12-well plates at 4×10^4 per well in 10% FBS/DMEM-H and incubated overnight. Hybridization of the siRNA was done in Dharmacon universal buffer by heating the solutions to 90 °C in a Perkin-Elmer PCR machine and then gradually cooling them to 30 °C for 30 min. Complexation of the double-stranded siRNA with the cationic lipid Lipofectamine 2000 (Invitrogen) was done according to the manufacturer's standard procedure. The oligonucleotides bound to cationic lipids were mixed in 10% FBS/DMEM-H and incubated with cells at 37 °C for 4 h; media was then removed and replaced with 2% FBS/DMEM-H, and the cells were incubated an additional 68−72 h. This technique, as well as those described below, is based on previous studies from our group.[52−54] The sequences of the siRNA oligonucleotides used are shown in Figure 2. Most of the work was done with the sequence designated ORF1, while some experiments were done with ORF2.

2.9. Cytotoxicity. NIH 3T3-MDR cells were treated with Lipofectamine 2000 complexes of standard or chemically modified siRNA oligos as described above. The cells were then replated onto new 12-well plates and incubated overnight followed by the addition of various concentrations of doxorubicin (Adriamycin) for 24 h. The drug and control medium was then removed and replaced with fresh drug-free 2%FBS/DMEM-H, and the cells were incubated an additional 48 h. Cells were then washed with PBS, harvested with trypsin-EDTA, and resuspended in 1 mL of a complete medium. The final cell number was enumerated by using an electronic particle counter (Particle Data, Elmhurst, IL). The relative increase in cell number was calculated as a percentage of untreated cells, and ID50 was determined by interpolation of plotted data.

2.10. Immunostaining of P-Glycoprotein. The level of cell surface expression of P-glycoprotein was studied by immunostaining using a flow cytometry assay. After treating NIH 3T3-MDR cells with standard or chemically modified siRNA complexes as described above, the cells were washed with PBS, trypsinized, resuspended in a complete medium, and washed again with PBS after centrifugation. The cells were counted for normalization, diluted to 6×10^5 total cells, and incubated with 17F9 (BD-Pharmingen) R-Phycoerythrin (R-PH)-conjugated mouse anti human P-glycoprotein monoclonal antibody in PBS for 30 min at 4 °C and then washed 2 times in 10% FBS/PBS. The levels of immunostaining by R-Phycoerythrin in viable cells (identified by light scattering) were then quantified on a Becton Dickinson flow cytometer using Cicero software (Cytomation, Fort Collins, CO).

2.11. Rhodamine 123 Accumulation. The fluorophore Rhodamine 123 is a substrate for the P-glycoprotein efflux pump; thus, Rhodamine 123 accumulation is often used as a surrogate for drug uptake.[53] NIH 3T3-MDR cells were treated with complexed CeNA siRNA oligos as described above. After 72 h the cells were trypsinized and suspended

(43) Esnouf, R. M. *Acta. Crystallogr.* **1999**, *D55*, 938−940.
(44) Kraulis, P. J. *J. Appl. Crystallogr.* **1991**, *24*, 946−950.
(45) Merritt, E. A.; Bacon, D. J. *Methods Enzymol.* **1997**, *277*, 505−524.
(46) Schmidt, M. W.; Baldridge, K. K.; Boatz, J. A.; Elbert, S. T.; Gordon, M. S.; Jensen, J. H.; Koseki, S.; Matsunaga, N.; Nguyen, K. A.; Su, S.; Windus, T. L.; Dupuis, M.; Montgomery, J. A., Jr. *J. Comput. Chem.* **1993**, *14*, 1347−1363.
(47) Bayly, C. I.; Cieplak, P.; Cornell, W. D.; Kollman, P. A. *J. Phys. Chem.* **1993**, *97*, 10269−10280.
(48) Wang, J.; Cieplak, P.; Kollman, P. A. *J. Comput. Chem.* **2000**, *21*, 1049−1074.
(49) Bradbrook, G. M.; Gleichmann, T.; Harrop, S. J.; Habash, J.; Raftery, J.; Kalb, J.; Yariv, J.; Hillier, I. H.; Helliwell, J. R. *J. Chem. Soc., Faraday Trans.* **1998**, *94*, 1603.
(50) Parker, J. S.; Roe, S. M.; Barford, D. *Nature* **2005**, *343*, 663−333.
(51) Pearlman, D. A.; Case, D. A.; Caldwell, J. W.; Ross, W. R.; Cheatham, T. E.; DeBolt, S.; Ferguson, D.; Seibel, G.; Kollman, P. *Comput. Phys. Commun.* **1995**, *91*, 1−41.
(52) Xu, D.; McCarty, D.; Fernandes, A.; Fisher, M.; Samulski, R. J.; Juliano, R. L. *Mol. Ther.* **2005**, *11*, 523−530.
(53) Kang, H.; Fisher, M. H.; Xu, D.; Miyamoto, Y. J.; Marchand, A.; Van Aerschot, A.; Herdewijn, P.; Juliano, R. L. *Nucleic Acids Res.* **2004**, *32*, 4411−4419.
(54) Xu, D.; Kang, H.; Fisher, M.; Juliano, R. L. *Mol. Pharmacol.* **2004**, *66*, 268−275.

in 10% FBS/DMEM-H. The cells were washed once and resuspended in a complete medium and warmed to 37 °C before adding Rhodamine 123 (1 μg/mL). After 1 h at 37 °C, cells were washed once with cold PBS and resuspended in PBS. The accumulation of Rhodamine 123 inside viable cells was measured by flow cytometry as described above.

2.12. RNA Extraction and Real-Time RT-PCR. Total RNA was isolated using a Tri Reagent kit (Molecular Research Center, Inc), and cDNA was synthesized from total RNA using an oligo-dT primer. Primers (Oligonucleotide Synthesis Core Facility, University of North Carolina) and probes (Integrated DNA Technologies, Santa Clara, CA) were designed using Primer 4 software and were designed to span exon−intron junctions. MDR1 probes were labeled at the 5′ end with the reporter dye 5-carboxyfluorescein and at the 3′ end with the quencher dye 5-carboxytetramethylrhodamine. The human glyceraldehyde 3-phosphate dehydrogenase (GAPDH) probe was labeled at the 5′ end with the reporter dye tetrachloro-6-carboxyfluorescein and at the 3′ end with the quencher dye 5-carboxytetramethylrhodamine. For MDR1, the sequences are as follows: probe, 5′-TCAGTAGCGATCT-TCCCAGCACCT-3′; sense primer, 5′-GTCTGGACAAGCACTGAAA-3′; antisense primer, 5′-AACAACGGTTCGGAAGTTT-3′. For human GAPDH, the sequences are as follows: probe, 5′-CAAGCTTCCCGT-TCTCAGCC-3′; sense primer, 5′-ACCTCAACTACATGGTTTAC-3′; antisense primer, 5′-GAAGATGGTGATGGGATTTC-3′. PCR reactions of cDNA samples and standards were performed with the use of Platinum Quantitative PCR SuperMix-UDG (Invitrogen) in a total reaction volume of 15 μL. Real-time PCR was performed using the ABI PRISM 7900 sequence detection system (Applied Biosystems, Foster City, CA). The PCR conditions were 50 °C for 2 min, 95 °C for 2 min, followed by 40 cycles of 95 °C for 15 s and 56 °C for 1.5 min. Standard curves were constructed with a PCR-II TOPO cloning vector (Invitrogen) containing the same fragment as that amplified by the Taqman system. The expression in each sample was calculated based on standard curves generated for MDR1 or GAPDH. Samples were normalized by dividing the copies of MDR1 by the copies of human GAPDH.

2.13. Nuclease Stability. For nuclease stability experiments, unmodified or CeNA modified siRNA duplexes were incubated either with partially purified nucleases or with 10% FBS. Thereafter the material was analyzed on 3% agarose/ethidium bromide gels in BPB/XC loading buffer and electrophoresed at 100 V for 45 min, and residual duplexes were imaged by ultraviolet illumination.

3. Results

3.1. Structure Determination by NMR spectroscopy of the Ce(5′-GCGTAGCG-3′)/r(5′-CGCUACGC-3′) Duplex. To investigate the structural characteristics of a CeNA:RNA duplex, high-resolution NMR studies were undertaken. In previous studies, it was shown that a cyclohexenyl nucleoside is a flexible molecule that can adopt different conformations when incorporated into different sequences. When incorporated in a self-complementary DNA dodecamer with sequence d(5′-CGCGA)c(A)d(TTCGCG-3′), a $_2H^3$ (N-Type) conformation of the cyclohexenyl nucleoside was observed.[5] In a modified DNA duplex consisting of d(5′-GCG)Ce(T)d(GCG-3′) hybridized with d(5′-CGCACGC-3′), the cyclohexenyl nucleoside was shown to occur in a $^2H_3$ (S-Type) conformation.[8] Here we wanted to investigate the behavior of the cyclohexenyl nucleosides in a CeNA:RNA duplex. The atom numbering, chemical structure, and main torsion angles of the CeNA strand are defined in Figure 3.

Using techniques as described in the Materials and Methods section NMR spectra were recorded and assigned. Subsequently, structural restraints were obtained. Various experimental results show the formation of a stable A-like helix in the modified and unmodified regions. The thermal stability of imino protons is characteristic for stable base pairing in the central part of the duplex that includes the modified site(s). Typical NOE interactions of the base protons with a continuous aromatic-to-anomeric and aromatic-to-aromatic proton walk could be observed throughout the complete helix and are indicative of regular base-stacking in an A-like helical structure. NMR spectroscopic information about the duplex backbone indicates a regular A-like conformation of the backbone. This duplex shows strong scalar couplings between P and H3′ of the previous residue and between P and H4′ of the next residue, and all phosphorus resonances show regular chemical shifts.

Table 1. Structure Determination Statistics for Each Set of 25 Structures after Refinement with All Experimental Restraints and Hydrogen Bonding between Base Pairs

	all restraints
total energy (kcal mol^{-1})	123 ± 7.3
NOE violations (>0.5 Å)	0
dihedral violations (>5°)	0 ± 0
rmsd from distance restraints (Å)	0.017 ± 0.007
rmsd from dihedral restraints (deg)	0.143 ± 0.037
rmsd from average structure for all heavy atoms (Å)	0.423 ± 0.120

Table 2. Backbone Torsion Angles and Helix Parameters of the RNA/CeNA Duplex

	A-DNA	B-DNA	CeNA strand	RNA strand
α (deg)	−50	−46	−72	−70
β (deg)	−172	−147	−178	−183
γ (deg)	41	36	58	55
δ (deg)	79	157	78	86
ϵ (deg)	−146	−205	−159	−156
ζ (deg)	−78	−96	−73	−67
χ (deg)	−165	−98	−165	−170
bp-slide (Å)	−1.75	−0.33	−1.59	
bp-twist (deg)	31.5	35.8	32.2	
h-rise (Å)	2.9	3.3	3.0	
h-twist (deg)	31.1	36.1	33	
inclination (deg)	12.0	2.4	9.1	
x-displacement (Å)	4.10	0.8	3.8	
minorgroove width (Å)	16.9	11.7	16.2	
major groove width (Å)	12.3	16.9	11.3	

To calculate the structure of the modified duplex we performed torsion angle molecular dynamics[37] followed by a refinement of 25 selected structures using the NMR-derived restraints in X-PLOR 3.851, as described in the Materials and Methods section. During the structure calculation experimental restraints were implemented to retain inter-proton distances, backbone torsion angles, and sugar conformations. During calculation, the structures converged to a family of structures with similar geometry (Figure 4). Structure determination statistics are listed in Table 1.

Inspection of the obtained structure shows that all the cyclohexenyl nucleosides occur in a $_2H^3$ conformation (N-Type) and that the overall helix structure is quite similar to an A-type duplex although some slight differences can be observed. A comparison of helix parameters and torsion angles of the RNA/CeNA duplex under study and standard A- and B-type helices can be found in Table 2.

It is clear that the helix parameters and torsion angles of the duplex more closely resemble those of a standard A-type helix than a standard B-type helix. It is however interesting to note that the twist is slightly larger than that of an A helix (RNA/

CeNA: 33; A-dsDNA: 31.1) and that the slide is decreased (RNA/CeNA: −1.59 Å; A-dsDNA: −1.75 Å). In the continuum of nucleic acid structures the RNA/CeNA duplex is thus situated between the A- and B-type helix, lying closer to the A- than to the B-type helix.[55,56] Deviation from the regular A-type structure is most pronounced for the α and the γ torsion angles. Although the duplex structure deviates from the A-form in the direction of the B-form, the groove widths are still very similar to that of the A-form of dsDNA.

3.2. Model Building. Figure 5A shows the model of the CeNA:RNA duplex bound to the PIWI protein (pdb in Supporting Information). A comparison of the Ligplot/HBPlus analysis[57−58] on both PIWI protein with bound siRNA:mRNA and CeNA:RNA does not show major differences in the interactions of the guide CeNA or RNA with the PIWI protein. All H-bonds/ionic bonds present in the X-ray structure are also present in the static model (Figure 5B). All specific interactions are with the phosphate backbone, providing no sequence specificity. The 2′-OH moieties present in siRNA but missing in the CeNA strand show no specific interaction with any PIWI residues. Although the six-membered sugar of CeNA is larger than a five-ring ribose, the backbone of sugar rings linked with phosphate groups is flexible enough to preserve an A-RNA-type conformation needed for hybridization with the mRNA (Figure 5C)

3.3. Biological Activity of CeNA Modified RNA Duplexes. As a biological model we chose to down regulate *MDR1*, a gene that is involved in cancer cell drug resistance. The gene product is the P-glycoprotein (Pgp) that is expressed on the cell surface. Pgp expression is monitored using a fluor-tagged anti-Pgp monoclonal antibody and flow cytometry. The siRNA mimics are transfected into the cells by standard means using Lipofectamine 2000. The siRNA sequences utilized are shown in Figure 2, with the sequence ORF1 used for most of the studies below. We have introduced cyclohexenyl-A and cyclohexenyl-G nucleotides in the sense and in the antisense strands of ORF1 at different locations (except the 5′-end of the antisense strand). A single cyclohexenyl nucleoside was incorporated at the 5′-end of the sense strand (oligonucleotide 2176) and at nucleotide position −6 (2177), −10 (2178), −17 (2179), and −18 (2181) of the sense strand (counting from the 5′-end). In the antisense strand, a modification was introduced at the −2 (2185), −4 (2186), −8 (2183) positions (counting from the 3′-end and not including the dTdT overhang). In three examples, two cyclohexenyl nucleosides were incorporated in the same sequence (2180 and 2182 of the sense oligonucleotide, and 2184 of the antisense oligo). The synthesized modified RNAs are given in Table 3.

In initial experiments, duplexes of CeNA modified oligonucleotides were formed with the complementary unmodified RNA and used as siRNAs at 50 nM. The percentage P-glycoprotein reduction was measured as described in Materials and Methods and compared with unmodified siRNA. In previous experiments we have shown that mismatched or "irrelevant" siRNAs do not affect P-glycoprotein expression levels.[54] The

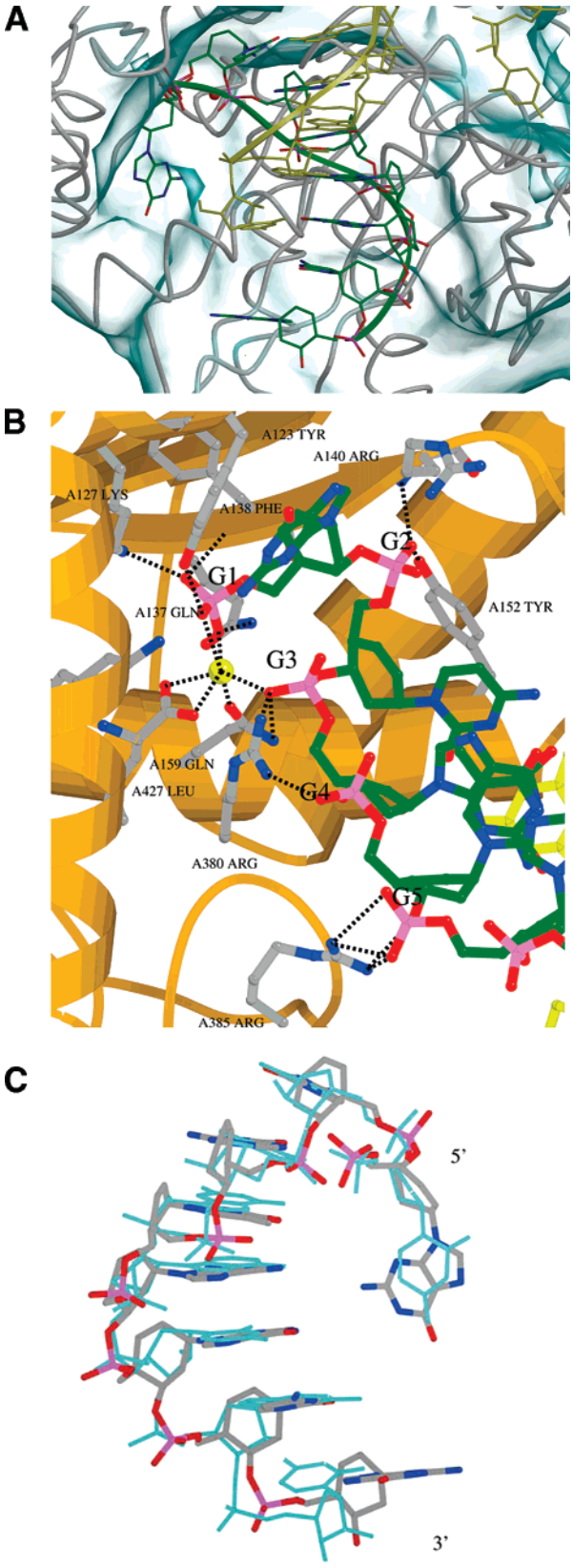

Figure 5. (A) Model of a CeNA:RNA guide:target duplex bound to a PIWI protein. The CeNA has CPK colors, mRNA is colored yellow, and the divalent metal Mn^{2+} is shown as a red ball. (B) Close-up of the interactions between the CeNA strand (green) and the PIWI protein. The Mn^{2+} metal is shown as a yellow sphere. Hydrogen bond interactions are represented as dotted lines. The mRNA is shown in yellow. (C) Overlay of CeNA (5′GCGTAGCG3′) (model) and guide RNA (5′GCGUAGCG3′) (X-ray structure, blue-green).

(55) Lescrinier, E.; Froeyen, M.; Herdewijn, P. *Nucleic Acids Res.* **2003**, *31*, 2975−2989.
(56) Nauwelaerts, K.; Lescrinier, E.; Herdewijn, P. *Chem.—Eur. J.* **2007**, *13*, 90−98.
(57) Wallace, A. C.; Laskowski, R. A.; Thornton, J. M. *Protein Eng.* **1995**, *8*, 127−134.
(58) McDonald, I. K.; Thornton, J. M. *J. Mol. Biol.* **1994**, *238*, 777−793.

Table 3. Modified Oligonucleotides That Were Used in the siRNA Experiment[a]

entry	sense oligonucleotide	MS calcd	MS found
	ORF1		
2176	5′-**G***UAUUGACAGCUAUUCGAAdTdT-3′	6645.9	6646.3
2177	5′-GUAUU**G***ACAGCUAUUCGAAdTdT-3′	6645.9	6646.4
2178	5′-GUAUUGACA**G***CUAUUCGAAdTdT-3′	6645.9	6646.5
2179	5′-GUAUUGACAGCUAUUC**G***AAdTdT-3′	6645.9	6646.2
2180	5′-GU**A***UUG**A***CAGCUAUUCGAAdTdT-3′	6640.0	6640.1
2181	5′-GUAUUGACAGCUAUUCG**A***AdTdT-3′	6645.9	6646.2
2182	5′-**G***U**A***UUGACAGCUAUUCGAAdTdT-3′	6640.0	6640.3
	ORF2		
2481	5′-GAACUCUUAGCGUAUGC**A***AdTdT-3′	6645.0	6645.5
2482	5′-GAACUCUU**A***GCGUAUGC**A***AdTdT-3′	6645.0	6645.6

entry	antisense oligonucleotide	MS calcd	MS found
	ORF1		
2183	5′-UUCGAAUAGCU**G***UCAAUACdTdT-3′	6605.9	6606.3
2184	5′-UUCGAAUAGCU**G***UCAAU**A***CdTdT-3′	6600.0	6600.6
2185	5′-UUCGAAUAGCUGUCAAU**A***CdTdT-3′	6606.0	6606.6
2186	5′-UUCGAAUAGCUGUCA**A***UACdTdT-3′	6606.0	6606.6
	ORF2		
2483	5′-UUGCAUACGCUAAG**A***GUUCdTdT-3′	6621.9	6622.5
2484	5′-UUGCAU**A***CGCUAAGAGUUCdTdT-3′	6621.9	6622.6

[a] Cyclohexenyl nucleotides are indicated in bold with asterisk.

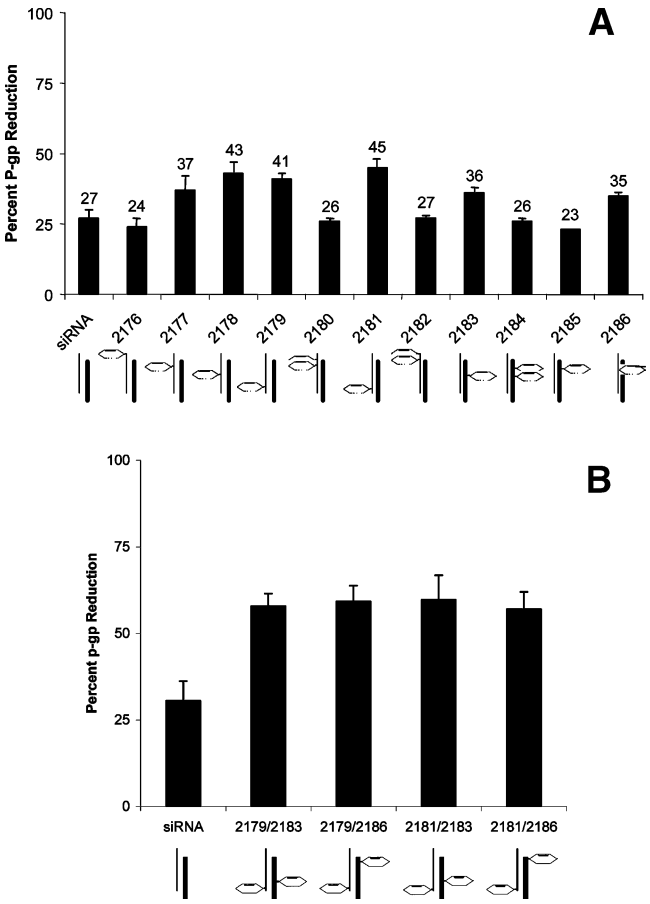

Figure 6. (A) Screen for siRNA effects on P-glycoprotein expression. NIH 3T3-MDR cells were treated with Lipofectamine 2000 and 50 nM unmodified or CeNA modified ORF1 siRNA. Cell surface P-glycoprotein expression in viable cells was evaluated by immunostaining and flow cytometry as described in Materials and Methods. The percentage reductions in P-glycoprotein expression were calculated on the basis of the fraction of the cell population shifted to greater than 1 standard deviation below the mean of the untreated controls. The mean and standard errors shown are derived from 3 experiments. Positions of CeNA modifications are indicated. (B) Effects of doubly modified siRNA on P-glycoprotein expression. NIH-3T3-MDR cells were treated with 50 nM CeNA modified or unmodified ORF1 siRNA duplexes, and cell surface P-glycoprotein expression in the viable cells were evaluated by flow cytometry. The mean and standard errors shown are derived from 3 experiments. Positions of CeNA modifications are indicated.

current results are given in Figure 6A. All CeNA containing duplexes show similar or increased biological activity when compared to the unmodified duplexes. This is most striking for duplexes containing the cyclohexenyl nucleoside in the middle section of the sense sequence (2177, 2178, 2179) and the antisense sequence (2183, 2186). Modifications in the end regions (2176, 2180, 2182, 2185) of both strands do not have a beneficial effect on the siRNA activity. 3′-end modification with cyclohexenyl nucleoside seems to be better accommodated in the sense sequence (2181) than in the antisense sequence (2185). Two oligonucleotide duplexes were selected for dose−response studies, one with a modified nucleoside in the sense sequence (2179) and another with the modified nucleoside in the antisense sequence (2186). The antisense modified siRNA shows increased efficacy while the sense modified siRNA became more efficacious at higher concentrations (data not shown).

Next, we examined whether the effect of modification of siRNA with cyclohexenyl nucleic acids is additive with modifications in both strands (Figure 6B). Equivalents of the G-modified RNAs 2179 and 2183 and the A-modified RNAs 2181 and 2186 were used for duplex formation. Also modified A/G mixed siRNAs were obtained by duplex formation between oligonucleotides 2179 and 2186, and 2181 and 2183. In all cases, the biological efficacy increased by about 2-fold (at 50 nM siRNA concentration) when compared with unmodified double-stranded RNA. Dose−response curves of two of these duplexes are shown in Figure 7.

In addition to studies on MDR-3T3 cells, a limited number of studies were carried out on drug-resistant human DX-5 cells. Here too an improved inhibition of P-glycoprotein expression was noted with the CeNA modified siRNAs. For example, where the unmodified siRNA at 50 nM resulted in an 11% reduction, the 2179/2183 CeNA compound gave a 29% reduction. Further, to ensure that the observed effects were not artifacts of a specific siRNA, we targeted MDR1 with a completely distinct sequence (ORF2, Figure 2) and examined effects of both unmodified and CeNa modified siRNAs having this sequence in MDR-3T3 cells. As seen in Table 4, at 50 nM CeNA modified ORF2 siRNAs consistently provided moderately enhanced suppression of P-glycoprotein expression as compared to the unmodified ORF2 siRNA.

The duplex 2179/2183 was also used to demonstrate that the reduction in P-glycoprotein expression is paralleled by a decrease in mRNA concentration. Total RNA was extracted from cells and quantified by real-time PCR. As can be observed in Figure 8A, the siRNAs with modifications in both strands indeed produce the greatest effect, similar to the results on protein expression.

Since P-glycoprotein expression leads to increased drug efflux and resistance against antitumor drugs, we evaluated whether the inhibition of P-glycoprotein expression results in a parallel increase in cytotoxic activity of such drugs, and if the inhibition of P-glycoprotein expression will result in increased accumula-

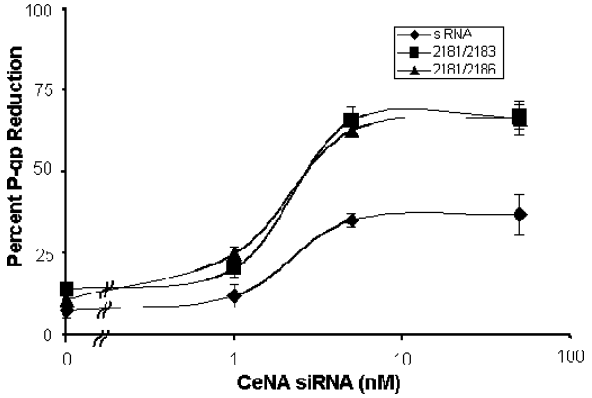

Figure 7. Dose−response effects of doubly modified siRNA on P-glycoprotein in NIH 3T3-MDR cells. Various concentrations of CeNA 2181/2183 and 2181/2186 modified duplex oligonucleotides were compared to unmodified ORF1 siRNA. Cell surface P-glycoprotein expression was measured by flow cytometry. The graph represents the mean and standard deviation of 3 measurements.

Table 4. Effects of ORF2 siRNAs on P-Glycoprotein Expression

oligonucleotides	percent reduction in Pgp expression
unmodified ORF2	44 ± 4
2481/2483	54 ± 1
2481/2484	64 ± 0.4
2482/2483	57 ± 3
2482/2484	57 ± 3

tion of substrate molecules in the cell. These results are shown in Figure 8B and C. The cells were first transfected with the unmodified, single modified (2186) and double modified (2179/2183) siRNA. After pretreatment with the siRNA, the cytotoxic effect of the antitumor drug doxorubicin (Adriamycin) was measured. Pretreatment with siRNA leads to an increase in the cytotoxicity of doxorubicin (Adriamycin) (a left shift of the dose−response curve), with the modified siRNA being more active than the unmodified siRNA. Rhodamine 123 is a fluorophore that is a good substrate for P-glycoprotein; thus Rhodamine 123 accumulation provides a convenient index of P-glycoprotein transport activity.[53] A parallel experiment measuring Rhodamine 123 uptake confirms the cytotoxicity data, i.e., that cells treated with CeNA modified siRNA are able to accumulate more Rhodamine 123 than ones treated with unmodified siRNA (Figure 8C).

As one potential contribution to the increased biological activity of CeNA modified siRNAs we have investigated their stability to nucleases. As seen in Figure 9, even introduction of a single CeNA unit in siRNA considerably increases stability to both purified nucleases and to the nucleases in serum.

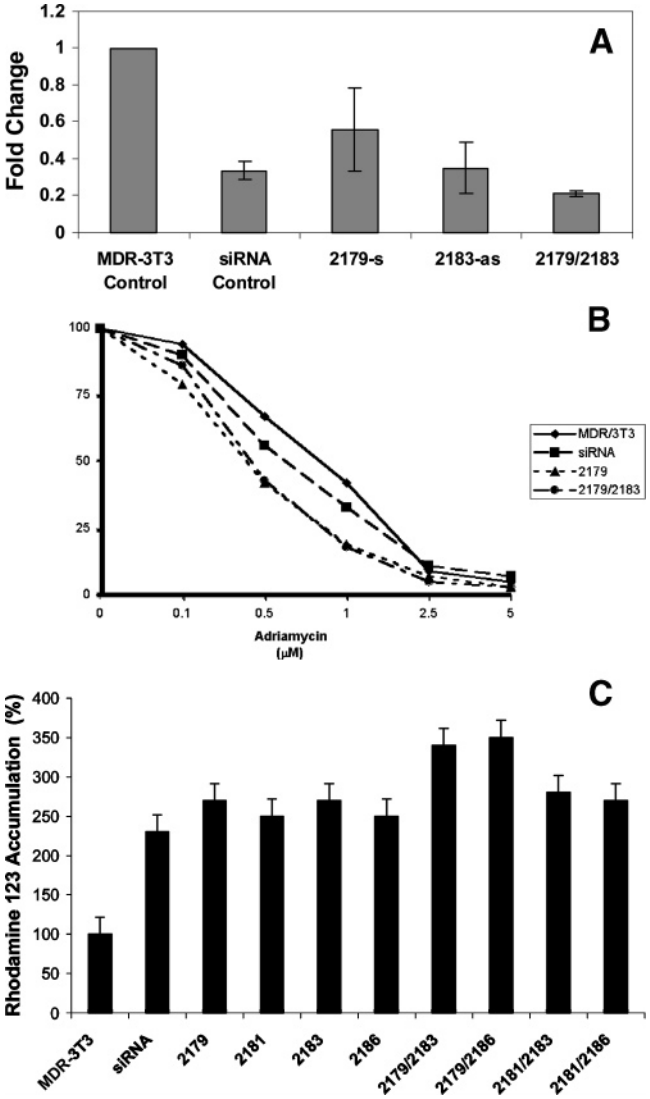

Figure 8. Real-time PCR analysis. MDR1 mRNA levels in NIH-3T3-MDR cells treated with 50 nM unmodified (siRNA control) or CeNA modified ORF1 siRNAs were quantified by real-time PCR. Values were normalized with those of GAPDH and expressed as a fold change over untreated cells. The graph represents the mean and standard deviation of 2 measurements. (B) Effects of CeNA siRNA on antitumor drug toxicity. NIH 3T3-MDR cells were transfected with unmodified ORF1 siRNA, modified oligo 2179, or modified duplex oligo 2179/2186 for 4 h and then grown for 72 h in 2% FBS DMEM-H. The cells were then exposed for 24 h to various concentrations of Adriamycin (doxorubicin). After a further 48 h in drug-free 2% FBS/DMEM-H medium, cell numbers were determined using a particle counter and the results were expressed as percent growth of the untreated control. (C) Effects of CeNA siRNACeNA oligos on Rhodamine 123 accumulation. NIH 3T3-MDR cells were treated with 50 nM unmodified or CeNA modified siRNA. Values of Rhodamine 123 uptake were measured, with the 100% level taken as that for untreated NIH 3T3-MDR cells. Mean and standard errors of 3 determinations are shown.

Discussion

In the search for oligonucleotides that can be used as RNA mimics, we have designed cyclohexenyl nucleic acids (CeNA) and have proven that CeNA forms stable duplexes with RNA and DNA.[3] When incorporating CeNA units in double-stranded DNA, we have demonstrated that the cyclohexenyl nucleoside can adopt different conformations (N-type and S-type) dependent on the number of incorporated cyclohexenyl residues, their location in the duplex, and the sequence of the duplex.[5,8] This shows that CeNA is not a highly conformational preorganized oligonucleotide but that it has some flexibility that might be important when being considered as a potential RNA mimic. Structural analysis of a natural nucleic acid duplex with one or two modified monomers incorporated gives detailed information about the conformation of the modified nucleoside (when present in a regular duplex) but will not give information about the duplex geometries of fully modified oligonucleotides that might be very useful in structure−activity relationship studies. Therefore, an NMR study was undertaken for a Ce(5′-GCGTAGCG-3′)/r(5′-CGCUACGC-3′) duplex. It is clear from this study that all the cyclohexenyl nucleosides occur in an N-type conforma-

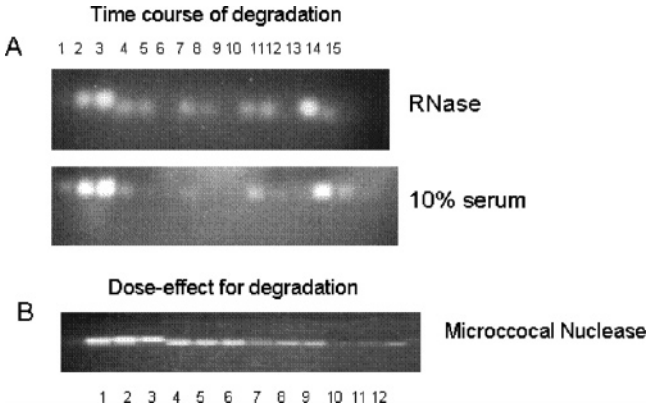

Figure 9. CeNA siRNA stability to Nucleases. (A) Oligonucleotides were incubated with pancreatic RNase or with fetal calf serum 10%. Pancreatic RNase incubations were 15', 30', 45'; 10% serum incubations were 12, 24, 72 h, all at room temperature. Residual intact oligonucleotide was resolved by gel electophoresis with ethidium bromide staining. Lanes 1−3, Load standard (90% degradation, 50% degradation, full load); lanes 4−6, S/AS unmodified ORF1 siRNA; lanes 7−9, 2179/AS siRNA; lanes 10−12, S/2183 siRNA; lanes 13−15, 2179/2183 siRNA. (B) Oligonucleotides were incubated with micrococcal nuclease for 30 min at 37 °C and analyzed as above. Lanes 1−3, unmodified siRNA, 2183, 2179/2183, no enzyme; lanes 4−6, unmodified siRNA, 2183, 2179/2183, 11 uμ/mL nuclease; lanes 7−9, unmodified siRNA, 2183, 2179/2183, 22 μg/mL nuclease; lanes 10−12, unmodified siRNA, 2183, 2179/2183, 33 μg/mL nuclease.

tion and that the overall structure is similar (but not identical) to an A-type duplex. A major question is whether the small deviation of the CeNA:RNA duplex from an RNA:RNA duplex is important for recognition of this duplex by the Argonaute protein, an issue which was investigated by molecular modeling using RNA as (target) a sense strand and CeNA as an antisense strand.

The PIWI domain of the Argonaute protein is an RNase H domain.[59,60] The crystal structure of the PIWI protein in complex with dsRNA, which mimics the 5′-end of an antisense RNA strand bound to the target mRNA, has been described.[50] This structure has been used as a model to investigate the binding fit between the PIWI protein and a CeNA:RNA duplex. An excellent fit in the energy minimized model has been observed between the geometries of dsRNA and the CeNA:RNA structure, as determined by NMR. All interactions between the dsRNA and the PIWI protein have also been observed for the CeNA:RNA duplex (Figure 6B). The model also confirms that the 2′-OH group of the guide oligonucleotide strand is not needed for binding to the protein. Structurally speaking, the CeNA:RNA duplex is a mimic of an RNA:RNA duplex and is most probably also recognized by proteins that recognize the RNA duplex.

A property that cannot be studied accurately by model building is whether CeNA can be considered as a functional mimic of RNA. Therefore, we have evaluated the influence of incorporation of CeNA nucleotides in an RNA duplex for siRNA applications, focusing on inhibition of the *MDR1* multidrug resistance gene as a target. Overall our experiments indicate that CeNA modifications are well-tolerated and for the most part provide moderate enhancements of activity over conventional siRNAs, as monitored by a reduction in expression of P-glycoprotein, the *MDR1* gene product. This is most pronounced when CeNA modifications are introduced in the middle sections of the duplex of either the sense or antisense strand. More interesting, however, is the additive effect of introduction of single CeNA modifications in both strands of the RNA duplex. Real-time PCR analysis demonstrates a specific decrease in MDR1 mRNA that parallels the observed reduction in P-glycoprotein expression. The introduction of CeNA modifications in the anti-MDR1 siRNA also results in increased changes in biological activity, including Rhodamine123 uptake and doxorubicin (Adriamycin) sensitivity, that closely parallel the effects on P-glycoprotein levels. Thus the CeNA modified oligonucleotides have good potential as biologically active siRNAs.

It is not obvious why the CeNA modifications have a generally beneficial effect on siRNA function. It seems unlikely that overall changes in helix stability are involved since the effect of a single CeNA substitution is small. One of the reasons for the increased biological activity might be the increased stability of the CeNA-containing duplexes to serum and cellular nucleases. We found that introduction of a even single CeNA unit in the siRNA increased the enzymatic stability considerably. This increased stability may be one aspect of the biological effectiveness of CeNA modified siRNAs. However, there may be other factors involved, such as the shape and flexibility of the helix in the region of the CeNA modifications. Elucidation of the mode of action of fully and partially modified CeNA siRNAs will be the subject of further research.

In summary, when forming a duplex with RNA, CeNA demonstrates an A-type structure that deviates from the classical A-form dsRNA in twist, inclination, and *x*-displacement. A model demonstrates that the CeNA can replace RNA as the antisense guide strand in a PIWI−dsRNA duplex. The small deviations in the helix parameters do not prevent CeNA from being a functional RNA mimic. Rather, incorporation of CeNA units in the sense or antisense strand of siRNA targeting P-glycoprotein expression leads to significant increases in the biological effect.

Acknowledgment. This work was supported by a K. U. Leuven grant (GOA 2002/13) to P.H, and by National Institutes of General Medical Sciences grant P01GM059299 to R.L.J. The authors are indebted to Dr. Ping Gu for the synthesis of the cyclohexenyl oligonucleotides.

Supporting Information Available: siRNA sequences with two dT overhangs at the 3′-end, targeting the MDR1 gene (Figure 1S). RP HPLC analysis of the anion exchange purified siRNA oligonucleosides, used in this study (Figure 2S). Melting points (T_m) of the siRNA duplexes under study (Table 1S). pdf structure file of the CeNA/RNA duplex, as determined by NMR. This material is available free of charge via the Internet at http://pubs.acs.org.

JA067047Q

(59) Song, J.-J.; Smith, S. K.; Hannon, G. J.; Joshua-Tor, L. *Science* **2004**, *305*, 1434−1437.
(60) Ma, J.-B.; Yuan, Y.-R.; Meister, G.; Pei, Y.; Tuschl, T.; Patel, D. J. *Nature* **2005**, *434*, 666−670.